Determination of maximum doppler shift in reverberation chamber using level crossing rate

Determination of Maximum Doppler Shift in Reverberation Chamber using Level Crossing Rate

Xiaoming Chen*, Per-Simon Kildal*, Jan Carlsson+

*Signals and Systems Department, Chalmers University of Technology
Gothenburg, Sweden
xiaoming.chen@chalmers.se

+Electronics department SP Technical Research Institute of Sweden
Boras, Sweden

***Abstract*— Doppler spread has been observed in reverberation chambers (RC) with moving mode-stirrers. In this paper, we propose a simple method to determine the maximum Doppler frequency shift in the RC by using level crossing rate (LCR). The Doppler spread bandwidth is twice of the maximum Doppler frequency. RC loading effect on Doppler spread is also studied in this paper. Using the method, it is found that maximum Doppler spread bandwidth tends to reduce when lossy objects are located into the RC, and the larger reduction the more larger lossy objects.**

I. Introduction

Reverberation chambers were traditionally used for electromagnetic compatibility (EMC) measurements, but during the past decade it has found new applications for measuring Over-The-Air (OTA) performance of small antenna and wireless devices in multipath environment. The reverberation chamber (RC) is basically a metal cavity, which is stirred to emulate a Rayleigh fading environment [1]. It has been used to measure antenna radiation efficiency, diversity gains and capacity of MIMO systems [2]. It can also be used to measure total radiated power [3] and total isotropic sensitivity [4] of active wireless devices and stations. The latter quantity may be affected by coherence bandwidth (or delay spread), and Doppler spread (or coherence time) of the propagation channels in the RC. Therefore, it is of importance to characterize these channel parameters. Coherence bandwidth in RC was studied in [5]; and Doppler spread in RC was studied in [6], [7]. In [6] it was shown that Doppler spread can be determined by step-wise stationary stirring. The characterization in [6] was done in terms of RMS Doppler bandwidth. This was introduced in [8], [9]. However, the relationship between RMS Doppler bandwidth and maximum Doppler shift depends on the shape of the Doppler spectrum, which in turn depends on angular distribution of incident waves and the radiation pattern of the antenna [10]. The maximum Doppler shift in RC was derived in [7] based on independent sample number in RC. However, the independent sample number in RC cannot be accurately estimated. Moreover, the measured average power by sweeping intermediate frequency (IF) bandwidth of the vector network analyzer (VNA) in [7] did not result in a unique value of the maximum Doppler shift.

In this paper, we generate the Doppler spread in the same way as in [6] by constructing a continuous time variation from a stepped stationary time response., but we herein instead use level crossing rate (LCR) to determine the maximum Doppler shift. According to the Doppler spread bandwidth definition [11], it is equal to twice the maximum Doppler shift. In addition, we use different lossy objects (loadings) inside the RC. The loading effect (via LCR) on Doppler spread is also studied in this paper.

II. Theory

A. Doppler Spread

We denote the channel transfer function $H(f,t)$. Then, its time autocorrelation function is

$$R_H(f,\partial t) = E[H^*(f,t)H(f,t+\partial t)] \tag{1}$$

where E represents expectation. Denoting ρ the Doppler frequency, the Doppler spectrum becomes [8]

$$D(f,\rho) = \int_{-\infty}^{\infty} R_H(f,\partial t)\exp(-j2\pi\rho\partial t)d(\partial t) \tag{2}$$

Doppler spread B_D is defined as the range of Doppler frequency ρ over which $D(f,\rho)$ is above a certain threshold [8]. The autocorrelation function (1) is equivalent to

$$R_H(f,\partial t) = H(f,\partial t)\otimes H^*(f,-\partial t) \tag{3}$$

where ⊗ represents convolution. Applying Fourier transform to both sides of (3), we easily obtain [6], [9]

$$D(f,\rho) = H(f,\rho)H^*(f,\rho) = |H(f,\rho)|^2 \tag{4}$$

where $H(f,\rho)$ is the Fourier transform of $H(f,t)$ w.r.t. time *t*, and the superscript * represents complex conjugation.

B. Level Crossing Rate

The LCR is defined as the rate at which the envelope of the signal crosses the level R in the downward direction [11]. It is a second-order channel statistic that is robust in different fading environments [12]. In Rician fading environments, LCR is [11]

$$L_R = \sqrt{2\pi(K+1)}\rho_m r \exp[-K-(K+1)r^2] I_0(2r\sqrt{K(K+1)}) \quad (5)$$

where K is Rician K-factor, defined as the ratio of line-of-sight (LOS) power to scattering power, ρ_m is the maximum Doppler shift, $r = R/R_{rms}$ where R_{rms} is the root mean square (RMS) of the signal, and I_0 is the modified Bessel function of 0*th* order. When K = 0 (the fading channel is Rayleigh), (5) simplifies to

$$L_R = \sqrt{2\pi}\rho_m r \exp(-r^2) \quad (6)$$

This K = 0 case will be a good approximation for our case because the K-factor is very small due to platform stirring [14].

III. Measurements and Results

The RC used in this paper is the Bluetest reverberation chamber, with a size of 1.75 m × 1.25 m × 1.8 m. A drawing of it is shown in Fig. 1. In Bluetest RC, there are three wall antennas mounted at three orthogonal walls used for polarization stirring [13]. The antenna under test (AUT) is placed on a platform, which will rotate during measurements, referred to as platform stirring [14]. Two metal plates are used as mechanical plate stirrers, corresponding to the mode-stirrers in other RCs. In the measurements, the platform and the two plates are set to move to 1000 positions simultaneously, evenly along the total distance they can move. At each stirrer position and for each of the three wall antennas, a full frequency sweep is performed by the vector network analyzer (VNA). The whole procedure is repeated for three loading conditions. They are specified as: *load0* corresponds to unloaded RC; *load1* is a head phantom filled with brain equivalent liquid; *load2* is the head phantom plus three Polyvinyl Chloride cylinders filled with microwave absorbers.

A. Doppler Spread in RC

The channel transfer function $H(f,t)$ is equal to the S-parameter $S_{21}(f,t)$ measured with a VNA under stationary conditions, i.e. when the stirrers are fixed, corresponding to constant time t. Such stationary measurements can then be repeated for different time t_n, corresponding to different fixed stirrer positions s_n, with $n = 1,\ldots N$ for all the stirrer positions. Although each of these S-parameters are measured under stationary conditions without Doppler shift, we can readily obtain the time varying S-parameter $S_{21}(f,t)$ by assuming the stirrers move "continuously" along all the stirrer positions with a certain speed. Equation (4) involves less computation compared with (2) from measured channel transfer functions.

Fig. 2 shows the Doppler spectrums calculated by (2)-(4) by using the approach in [6] and by assuming that it takes the stirrers in RC T = 0.2 sec to go through all the 1000 stirrer positions. It shows that Doppler spread is larger at higher frequencies, and that Doppler spread is smaller with heavier RC loading. However, it is difficult to determine the maximum Doppler shift from the Doppler spectrum. We thereby introduce LCR method to determine the maximum Doppler shift using (5). Thus, K-factor in the RC must be determined a priori.

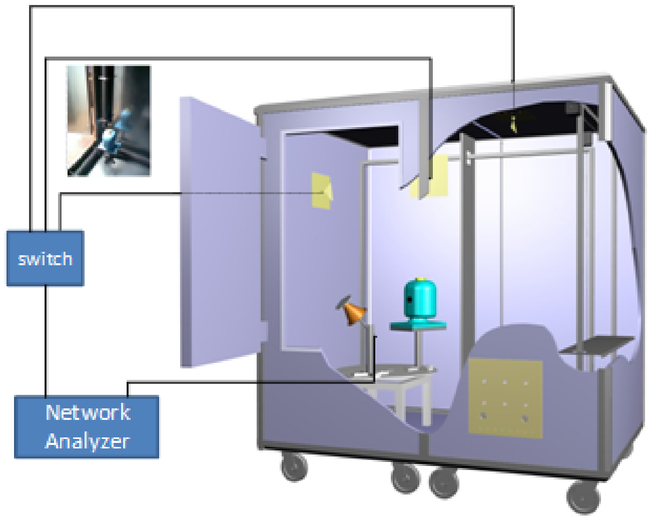

Fig. 1 Drawing of Bluetest RC with two mechanical plate stirrers, one platform and three wall antennas (The inserted little photo in the upper left corner shows the head phantom and the location of the three absorber-filled PVC cylinders of *load2* configuration.)

B. Rician K-factor in RC

It was shown in [15] that RC can be used to emulate Rician fading environments with a K-factor.

$$K = \frac{P_d}{P_s} = \frac{|\overline{S_{21}}|^2}{\overline{|S_{21} - \overline{S_{21}}|^2}} \quad (7)$$

where P_d is the power of the LOS component $\overline{S_{21}}$ of the total transfer function S_{21}, and P_s is the averaged power of the statistical scattering component of S_{21}, and the overhead bar represents average over all the samples. The average mode bandwidth of the RC, introduced in [16] based on Hill's transmission formula [17], is given as,

$$\Delta f = \frac{c_0^3 e_{rad1} e_{rad2}}{16\pi^2 V f^2 P_s} \quad (8)$$

The LOS power can be written, using Friis formula, as

$$P_d = (\frac{\lambda}{2\pi r})^2 G_1 G_2 = (\frac{c}{4\pi r f})^2 D_1 D_2 e_{rad1} e_{rad2} \quad (9)$$

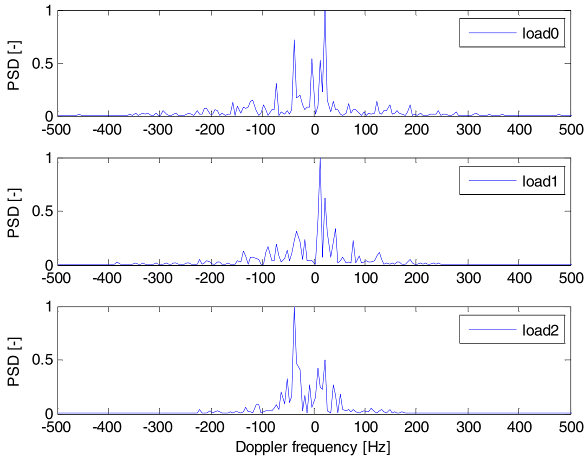

(a)

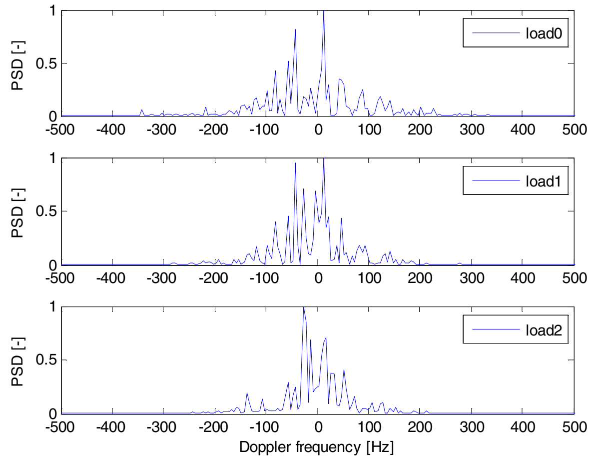

(b)

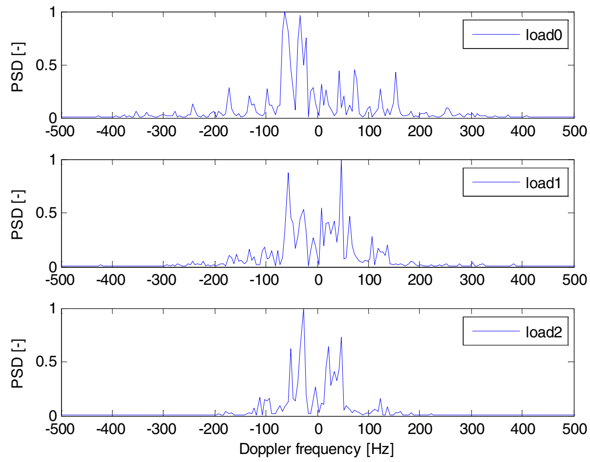

(c)

Fig. 2. Doppler spectrums for different loadings at 1.7 GHz (a), 2.2 GHz (b) and 2.7 GHz (c) by assuming the stirrers go through all the 1000 positions in 0.2 sec.

where G_1, G_2, D_1, D_2, e_{rad1} and e_{rad2} are antenna gains, directivities and radiation efficiencies of transmitting and receiving antennas respectively. Combining (7)-(9),

$$K = \frac{VD_1 D_2}{cr^2}\Delta f \quad (10)$$

Equation (10) shows that K-factor is proportional to average mode bandwidth, which depends on RC loading [5]. Provided that the number of independent values of the statistical part of the channel is large enough, the K-factor in the RC is mainly determined by RC loading.

K-factor should be calculated using (7) over all the stirrer positions. Fig. 3 shows the K-factor as a function of frequency for different loading conditions. Due to the platform stirring [14], the K-factor levels for the different loading conditions are similar. Note that without platform stirring, K-factor will increase as increasing loading [15].

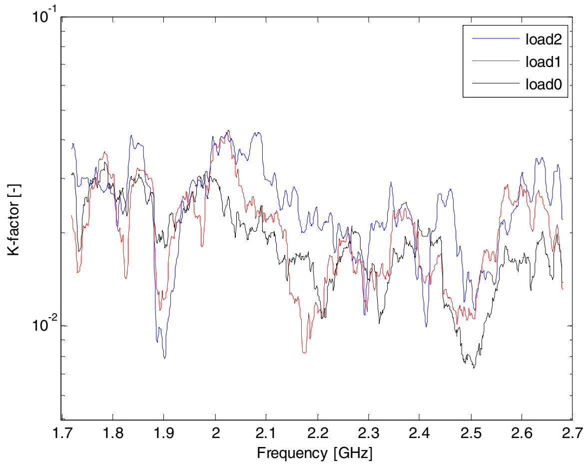

Fig. 3. K-factor in RC at *load0*, *load1* and *load2*.

C. Maximum Doppler Shift in RC

As shown from Fig. 2, Doppler spread shrinks as RC loading increases. However, it is difficult to determine the maximum Doppler shift from the Doppler spectrum uniquely. Therefore, we introduce LCR method, i.e. (5), to determine the maximum Doppler shift.

The LCR can be obtained from the 1000 stirrer position samples by counting how many times the S_{21} crosses a certain level R in the downward direction (or equivalently upward direction), then dividing the crossing number by T (20 sec). Different R will result in different LCR. The LCRs for different loading conditions are shown in Fig. 4.

The K-factor is shown in Fig. 3. Since the K-factors (due to platform stirring) for *load0-load2* are negligible, the maximum Doppler shift can be calculated using (6)

$$\rho_m = \frac{L_R}{\sqrt{2\pi} r \exp(-r^2)} \quad (11)$$

Fig. 5 shows the maximum Doppler shift obtained using LCR method. As expected, the maximum Doppler shift increases with increasing frequency; and it is largest for unloaded RC. Comparing with Fig. 2, the maximum Doppler shifts obtained using LCR agree well with the corresponding Doppler spectrums.

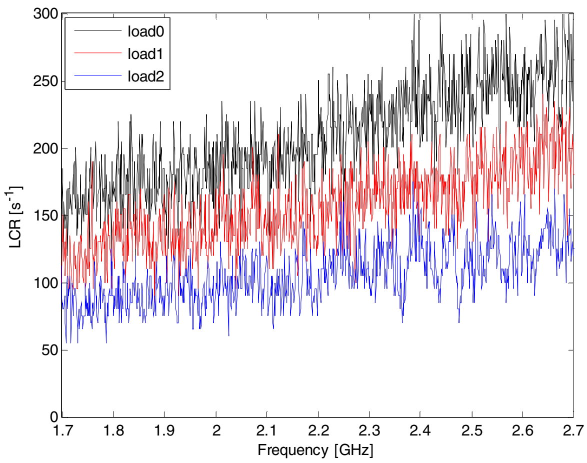

Fig. 4. LCRs in RC at *load0*, *load1* and *load2* by assuming the stirrers go through all the 1000 positions in 0.2 sec.

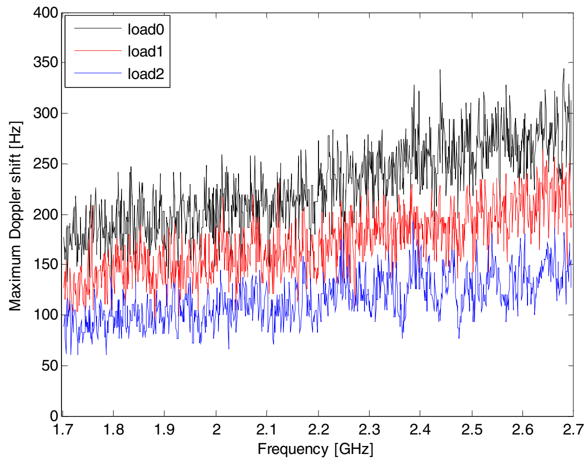

Fig. 5. Maximum Doppler shift in RC at *load0*, *load1* and *load2* by assuming the stirrers go through all the 1000 positions in 0.2 sec.

IV. Conclusions

We generate Doppler spreads in RC at different loading conditions using step-wise stationary stirring. We introduce LCR method to uniquely determine the maximum Doppler shifts. It is shown that the maximum Doppler shift obtained using the method agrees with corresponding Doppler spectrum well, and that maximum Doppler shift decreases with increasing loading of the RC.

Acknowledgment

This work has been supported in part by The Swedish Governmental Agency for Innovation Systems (VINNOVA) within the VINN Excellence Center Chase.

References

[1] J. G. Kostas and B. Boverie, "Statistical model for a mode-stirred chamber," *IEEE trans. Electromagn. Compat.,*vol.33, no. 4, pp. 366-370*,* Nov. 1991.

[2] K. Rosengren and P.-S. Kildal, "Radiation efficiency, correlation, diversity gain and capacity of a six-monopole antenna array for a MIMO system: theory, simulation and measurement in reverberation chamber," *IEE Proc. Microw. Antennas Propag.* vol. 152, pp. 7-16, 2005. See also Erratum published in August 2006.

[3] N. Serafimov, P-S. Kildal, T. Bolin, "Comparison between radiation efficiencies of phone antennas and radiated power of mobile phones measured in anechoic chambers and reverberation chamber", *IEEE AP-S International Symposium*, San Antonio, Texas, June 2002.

[4] C. Orlenius, P.–S. Kildal, and G. Poilasne, "Measurement of Total Isotropic Sensitivity and Average Fading Sensitivity of CDMA phones in Reverberation Chamber," *IEEE AP-S Internal Symp. Washington D.C.,* 3-8 July, 2005.

[5] X. Chen, P.-S. Kildal, C. Orlenius and J. Carlsson, "Channel sounding of loaded reverberation chamber for Over-the-Air testing of wireless devices - coherence bandwidth and delay spread versus average mode bandwidth", *IEEE Antennas and Wireless Propagation Letters*, vol. 8, pp. 678-681, 2009.

[6] K. Karlsson, X. Chen, P.-S. Kildal, J. Carlsson, "Doppler spread in reverberation chamber predicted from measurements during stationary step-wise stirring", Antennas and Wireless Propagation Letters, Vol. 9, pp. 497 - 500, 2010.

[7] P. Hallbjörner, A. Rydberg, "Maximum Doppler frequency in reverberation chamber with continuously moving stirrer," *Loughborough antenna and propagation conference*, 2007.

[8] S. Stein, "Fading channel issues in system engineering," *IEEE Journal on selected areas in communications*, vol. 5, no. 2, pp. 68-89, Feb. 1987.

[9] S. J. Howard, K. Pahlavan, "Doppler spread measurement of indoor radio channel," *Electronic letters*, vol. 26, no. 2, pp. 107-109, Jan. 1990.

[10] P. Petrus, J. H. Reed and T. S. Rappaport, "Effects of directional antennas at the base station on the Doppler spectrum", *IEEE Commun. Lett.*, vol. 1, pp. 40-42, Mar. 1997.

[11] A. Goldsmith, *Wireless Communications*, Cambridge university press, 2005.

[12] A. Abdi, K. Wills, H. A. Barger, M. S. Alouini and M. kaveh, "Comparison of the level corssing rate and average fade duration of Rayleigh, Rice and Nakagami fading models with mobile channel data", *IEEE Veh. Tech. Conf.*, pp. 1850-1857, 2000.

[13] P-S. Kildal, C. Carlsson, "Detection of a polarization imbalance in reverberation chambers and how to remove it by polarization stirring when measuring antenna efficiencies", *Microwave and Optical Technology Letters, Vol.* 32, No 2, pp. 145-149, July 2002.

[14] K. Rosengren, P-S. Kildal, C. Carlsson, J. Carlsson, "Characterization of Antennas for Mobile and Wireless Terminals in Reverberation Chambers: Improved Accuracy by Platform Stirring", *Microwave and Optical Technology Letters,* Vol. 30, No 20, pp 391-397, Sept. 2001.

[15] C. L. Holloway, D. A. Hill, J. M. Ladbury, P. F. Wilson, G. Koepke, and J. Coder, "On the Use of Reverberation Chamber to Simulate a Rician Radio Environment for the Testing of Wireless Devices," *IEEE Trans. on antennas and propagation, vol. 54, No. 11*, pp. 3167-3177, Nov. 2006.

[16] U. Carlberg, P.-S. Kildal, and J. Carlsson, "Study of antennas in reverberation chamber using method of moments with cavity Green's function calculated by Ewald summation," *IEEE Trans. Electromagn. Compat.*, vol. 47, no.4, pp. 805-814, Nov. 2005.

[17] D. A. Hill, M. T. Ma, A. R. Ondrejka, B. F. Riddle, M. L. Crawford, and R. T. Johnk, "Aperture Excitation of Electrically Large, Lossy Cavities," *IEEE trans. Electromagn. Compat., vol.36, no. 3, pp169-178,* Aug. 1994.